Journal for ImmunoTherapy of Cancer

Higher proportions of CD39+ tumor-resident cytotoxic T cells predict recurrence-free survival in patients with stage III melanoma treated with adjuvant immunotherapy

Grace Heloise Attrill ,[1,2] Carina N Owen,[1,3] Tasnia Ahmed,[1] Ismael A Vergara,[1,2] Andrew J Colebatch,[1,4] Jordan W Conway,[1,2] Kazi J Nahar,[1,2] John F Thompson ,[1,5] Ines Pires da Silva ,[1,6] Matteo S Carlino,[1,6] Alexander M Menzies,[1,7] Serigne Lo ,[1,2] Umaimainthan Palendira ,[2] Richard A Scolyer ,[1,4] Georgina V Long ,[1,7] James S Wilmott [1,2]

To cite: Attrill GH, Owen CN, Ahmed T, *et al*. Higher proportions of CD39+ tumor-resident cytotoxic T cells predict recurrence-free survival in patients with stage III melanoma treated with adjuvant immunotherapy. *Journal for ImmunoTherapy of Cancer* 2022;**10**:e004771. doi:10.1136/jitc-2022-004771

► Additional supplemental material is published online only. To view, please visit the journal online (http://dx.doi.org/10.1136/jitc-2022-004771).

RAS, GVL and JSW contributed equally.

Accepted 04 May 2022

For numbered affiliations see end of article.

Correspondence to
Dr James S Wilmott;
james.wilmott@sydney.edu.au

ABSTRACT

Background Adjuvant immune checkpoint inhibitor (ICI) immunotherapies have significantly reduced the recurrence rate in high-risk patients with stage III melanoma compared with surgery alone. However, 48% of anti-PD-1-treated patients will develop recurrent disease within 4 years. There is a need to identify biomarkers of recurrence after adjuvant ICI to enable identification of patients in need of alternative treatment strategies. As cytotoxic T cells are critical for the antitumor response to anti-PD-1, we sought to determine whether specific subsets were predictive of recurrence in anti-PD-1-treated high-risk patients with stage III melanoma.

Methods Associations with recurrence in patients with stage III melanoma were sought by analyzing resection specimens (n=103) taken prior to adjuvant nivolumab/pembrolizumab±low-dose/low-interval ipilimumab. Multiplex immunohistochemistry was used to quantify intratumoral CD8+ T-cell populations using phenotypical markers CD39, CD103, and PD-1.

Results With a median follow-up of 19.3 months, 37/103 (36%) of patients had a recurrence. Two CD8+ T-cell subpopulations were significantly associated with recurrence. First, CD39+ tumor-resident memory cells (CD39+CD103+PD-1+CD8+ (CD39+ Trm)) comprised a significantly higher proportion of CD8+ T cells in recurrence-free patients (p=0.0004). Conversely, bystander T cells (CD39−CD103−PD-1−CD8+) comprised a significantly greater proportion of T cells in patients who developed recurrence (p=0.0002). Spatial analysis identified that CD39+ Trms localized significantly closer to melanoma cells than bystander T cells. Multivariable analysis confirmed significantly improved recurrence-free survival (RFS) in patients with a high proportion of intratumoral CD39+ Trms (1-year RFS high 78.1% vs low 49.9%, HR 0.32, 95% CI 0.15 to 0.69), no complete lymph node dissection performed, and less advanced disease stage (HR 2.85, 95% CI 1.13 to 7.19, and HR 1.29, 95% CI 0.59 to 2.82). The final Cox regression model identified patients who developed recurrence with an area under the curve of 75.9% in the discovery cohort and 69.5% in a separate validation cohort (n=33) to predict recurrence status at 1 year.

Conclusions Adjuvant immunotherapy-treated patients with a high proportion of CD39+ Trms in their baseline melanoma resection have a significantly reduced risk of melanoma recurrence. This population of T cells may not only represent a biomarker of RFS following anti-PD-1 therapy, but may also be an avenue for therapeutic manipulation and enhancing outcomes for immunotherapy-treated patients with cancer.

WHAT IS ALREADY KNOWN ON THIS TOPIC

⇒ Although adjuvant anti-PD-1 therapy has been highly effective in the treatment of metastatic melanoma, many patients experience melanoma recurrence following therapy. Due to their vital role in immunotherapy response, CD8+T-cell populations could act as potential biomarkers for recurrence and indicate mechanisms of immunotherapy resistance.

WHAT THIS STUDY ADDS

⇒ Of eight phenotypically distinct CD8+ T-cell populations infiltrating metastatic melanoma, we identified a CD39+CD103+PD-1+ population which was strongly associated with improved recurrence-free survival.

HOW THIS STUDY MIGHT AFFECT RESEARCH, PRACTICE AND/OR POLICY

⇒ This population could act as a predictive biomarker for recurrence and, since its phenotype is enriched for tumor reactivity, could potentially be targeted for emerging therapies.

INTRODUCTION

Immune checkpoint inhibitors (ICIs) have significantly advanced the treatment of many

cancers, particularly melanoma. Adjuvant pembrolizumab and nivolumab (anti-PD-1 ICI) significantly improve the recurrence-free survival (RFS) of patients with stage III melanoma over surgery alone[1] or adjuvant ipilimumab,[2] with a 3-year RFS of 64% for pembrolizumab compared with 44% for surgery alone.[3] Additionally, adjuvant ipilimumab (anti-CTLA-4 ICI) improves overall survival compared with surgery alone,[4 5] however, with significant toxicity. The combination of anti-PD-1 with anti-CTLA-4 in the neoadjuvant setting[6 7] or for resected stage IV disease[8] has demonstrated prolonged RFS, although a trial of adjuvant combination therapy of nivolumab with low-dose/low-interval anti-CTLA-4 was negative.[9] Regardless, in the adjuvant setting, a significant proportion of patients will experience disease recurrence and treatment-related toxicity will remain an important problem.[1 2 10–12] As such, predictive biomarkers are needed to stratify patients by their potential to recur in an attempt to better determine risk/benefit for individual patients, for example identifying patients who do not require adjuvant treatment and those who will recur following adjuvant anti-PD-1, who require additional treatments such as combination with BRAF/MEK inhibitors or alternative therapies to prevent recurrence in these high-risk patients.

While the exact mechanisms underpinning recurrence in ICI-treated patients remain unclear, much of the research into predictive biomarkers has focused on the patient immune response.[13] In recent years, the most widely used biomarker in this context has been tumor programmed death ligand-1 (PD-L1) expression.[14–17] The use of PD-L1 as a biomarker stems from trials which demonstrated that adjuvant anti-PD-1-treated patients with melanoma with PD-L1-positive tumors had a 3-year RFS of 65%, compared with 57% for patients with PD-L1-negative tumors.[3] However, patients with PD-L1-negative tumors still derived significant benefit from therapy compared with placebo. Therefore, PD-L1 expression is not routinely used as a biomarker to select treatment in melanoma. Forty-eight percent of melanomas have mutations in the BRAF gene, with the BRAF V600E mutation being the most common of these. Approximately 80% of tumors with this mutation are susceptible to targeted therapy with combined BRAF inhibitor and MEK inhibitor therapy.[18–22] Recent studies have also found that tumor mutation burden (TMB) and interferon gamma (IFN-γ) show promise as biomarkers for response to anti-PD-1+anti-CTLA-4 in the neoadjuvant setting,[7] and anti-PD-1 with or without anti-CTLA-4 in the advanced setting.[21] Investigation of TMB and IFN-γ has stemmed from the consistent demonstration of strong associations between increased CD8+ T-cell infiltration and improved response to anti-PD-1 therapy in patients with advanced-stage metastatic disease.[22 23] Further phenotyping of tumor-infiltrating CD8+T cells, particularly the expression of PD-1, CD103, and CD39, has revealed stronger associations with the anti-PD-1 response in patients with advanced stage melanoma than on CD8 T-cell numbers alone.[24] As well as being an immune checkpoint targeted by anti-PD-1 therapy, PD-1 is also upregulated by chronically antigen-experienced and potentially exhausted CD8+ T cells.[23 25] The integrin protein CD103 is understood to be a marker of tumor residency.[24] CD103 allows CD8+ T cells to be retained in inflamed tissues such as sites of infection and the tumor microenvironment (TME),[26] and as such, CD103+CD8+ T cells are termed 'tissue-resident memory cells (Trms)'.[27 28] CD39 has also gained interest in recent years due to its proposed role as a marker of specificity for tumor antigens when expressed by CD8+ T cells in the TME. Since this function is yet to be proven, and due to the fact that CD39 is often coexpressed with PD-1 and CD103, it is currently better described as a marker of tumor reactivity rather than antigen specificity.[29–31]

This study sought to determine the association of specific T-cell phenotypes with recurrence in patients with stage III melanoma treated with adjuvant anti-PD-1 monotherapy or combination anti-PD-1 and low-dose/low-interval anti-CTLA-4 therapy (n=103). The findings were validated in an independent cohort (n=33).

METHODS

Cohort and study design

A retrospective discovery cohort of consecutive patients with available resected stage III melanoma tissue—including both nodal and in-transit metastases—who were treated with adjuvant anti-PD-1 monotherapy or combination anti-PD-1 and anti-CTLA-4 therapies at Melanoma Institute Australia, Sydney, between May 2015 and December 2018 was collected (n=103, table 1). Of these, 77 received anti-PD-1 monotherapy and 26 received anti-PD-1 + very low-dose anti-CTLA-4 (1 mg/kg every 6 weeks) combination therapy. This dosage of combination therapy conferred no survival benefit compared with PD-1 monotherapy.[9] A subsequent validation cohort using identical selection criteria was identified for validation of a predictive model of recurrence (n=33). The validation cohort consisted of consecutive patients treated from January 2019 to December 2019 with available biospecimens. All patients in this cohort received anti-PD-1 monotherapy. The primary endpoint was melanoma recurrence following resection of the stage III tumor, with RFS defined as the time from adjuvant PD-1 treatment start to recurrence. Resected stage III melanoma tissues were fixed in 10% buffered formalin and embedded in paraffin. H&E-stained slides were reviewed by a pathologist (AJC) to assess the suitability of each sample for downstream multiplex fluorescent immunohistochemistry (mIHC). Samples were considered appropriate for analysis if there were at least 100 viable tumor cells on a given slide. Twelve patients (8.8%) lacked sufficient viable tumor cells and were excluded, leaving tissue from 124 patients available for analysis (discovery n=91, validation n=33). BRAF mutation status was determined using either IHC with the BRAF VE1 antibody (n=103)[32] or genetic testing (n=28). As only the V600E status could

Table 1 Clinicopathological characteristics of patient cohorts

Patient characteristics	Discovery (n=103)	Validation (n=33)
Age (years), mean (range)	59.9 (29.0–79.8)	65.2 (22.0–82.0)
Age (>median), n (%)		
≤60	54/103 (52.4)	10/33 (30.3)
>60	49/103 (47.6)	23/33 (69.7)
Sex, n (%)		
Female	35/103 (34.0)	8/33 (24.2)
Male	68/103 (66.0)	25/33 (75.8)
BRAF, n (%)		
non-V600E/WT	70/94 (74.5)	27/33 (81.8)
V600E	24/94 (25.5)	6/33 (18.2)
Time to stage III from primary melanoma (months), n (%)		
Concurrent	45/84 (53.6)	18/33 (54.5)
3–6 months	6/84 (7.1)	2/33 (6.1)
6 months–1 year	5/84 (6.0)	1/33 (3.0)
1–2 years	10/84 (11.9)	2/33 (6.1)
>2 years	18/84 (21.4)	10/33 (30.3)
Stage III, n (%)		
IIIA	9/103 (8.7)	0/33 (0)
IIIB	39/103 (37.9)	15/33 (45.5)
IIIC	54/103 (52.4)	17/33 (51.5)
IIID	1/103 (1.0)	1/33 (3.0)
Stage III detail, n (%)		
Nodal only	84/103 (81.6)	24/33 (72.7)
ITM only	14/103 (13.6)	6/33 (18.2)
Both nodal/ITM	5/103 (4.9)	3/33 (9.1)
LN status, n (%)		
Microscopic	40/89 (44.9)	9/27 (33.3)
Macroscopic	49/89 (55.1)	18/27 (66.7)
CLND performed, n (%)		
No	36/94 (38.3)	19/33 (57.6)
Yes	58/94 (61.7)	14/33 (42.4)
CLND site, n (%)		
Neck	17/58 (29.3)	3/14 (21.4)
Axilla	27/58 (46.6)	3/14 (21.4)
Groin	12/58 (20.7)	4/14 (28.3)
Multiple	2/58 (3.4)	4/14 (28.3)
Number of nodes involved, n (%)		
0–1	28/58 (48.3)	16/27 (59.3)
2–3	14/58 (24.1)	9/27 (33.3)
≥4	16/58 (27.6)	2/27 (7.4)
Extranodal spread, n (%)		
No	31/57 (54.4)	15/27 (55.6)
Yes	26/57 (45.6)	12/27 (44.4)
LDH (categorized), n (%)		
Normal	95/96 (99.0)	32/33 (97.0)
Elevated	1/96 (1.0)	1/33 (3.0)
PD-L1 status (>1%), n (%)		
Negative	64/102 (62.7)	11/30 (36.7)
Positive	38/102 (37.3)	19/30 (63.3)

*More than 10% of the data are missing for time to stage III.
CLND, completion lymph node dissection; ITM, intransit metastases; LN, lymph node.

be determined for the majority of patients, we classified BRAF mutation status as either V600E or non-V600E/WT.

PD-L1 and multiplex immunohistochemistry

Formalin-fixed paraffin-embedded tissue was cut at 3 µm thickness for mIHC or 4 µm thickness for PD-L1 IHC. Tissue was mounted on Superfrost Plus slides (Thermo Fisher Scientific) and air-dried overnight. Slides were then placed in a vacuum sealed dehydrator for short-term storage and removed immediately prior to staining. Investigators (GHA) were blinded to patient recurrence status throughout staining and image analysis.

Singleplex PD-L1 IHC was performed following deparaffinization, dehydration, and antigen retrieval in a pressurized decloaking chamber (Biocare Medical). Slides were placed in AR 9 buffer (Akoya Biosciences) and heated to 110°C for 20 min, then cooled to room temperature in a water bath. Staining was performed on a Dako Autostainer Plus (Agilent Technologies). First, endogenous peroxidase activity was blocked by incubating slides in 3% H_2O_2 (Sigma-Aldrich) for 10 min, then slides were incubated with the primary antibody for PD-L1 (Cell Signaling, E1L3N, 1:200) for 45 min. Slides were then incubated with Mach 3 Rabbit probe (Biocare Medical) for 20 min followed by Mach 3 Rabbit HRP (Biocare Medical) for 20 min. Slides were then incubated with Betazoid DAB Chromogen Kit (Biocare Medical) for 5 min and counterstained using Mayer's hematoxylin (Sigma-Aldrich) for 10 min. After a final rise with H_2O, slides were rehydrated and coverslipped. PD-L1 staining was interpreted and scored by a clinical pathologist (AJC). PD-L1 status was defined as positive if there was partial or complete membrane staining in at least 1% of tumor cells.[33]

Multiplex IHC staining was performed in an intelliPATH FLX Automated Slide Stainer (Biocare Medical). First, endogenous peroxidase activity was blocked by incubating slides in 3% H_2O_2 for 10 min, then slides were incubated in sequential rounds of primary antibody for either PD-1 (Abcam, EPR4877(2), 1:1500), CD103 (Abcam, EPR4166(2), 1:1500), CD8 (Dako, C8/144B, 1:1500), CD3 (Cell Marque, MRQ-39, 1:1500), CD39

(Abcam, EPR20627, 1:2000), or SOX10 (Biocare Medical, BC34, 1:200) for 30 min. Slides were then incubated with either Mach 3 Rabbit probe (Biocare Medical) for 10 min followed by Mach 3 Rabbit HRP (Biocare Medical) for 10 min, or Opal Polymer HRP Ms+Rb (Akoya Biosciences) for 30 min as outlined in online supplemental table 1. The slides were then incubated in Opal fluorophore (1:100) diluted in 1X Plus Amplification Diluent (Akoya Biosciences) for 10 min. Following each Opal detection, slides were stripped via antigen retrieval as previously mentioned before each antibody in the multiplex. Single color control, multiplex control, and unstained control slides were stained alongside patient samples to determine background staining and create a spectral library for spectral unmixing. Following the addition of Opal for the final antibody, the slides were incubated for 5 min with Spectral DAPI (1:2000, Akoya Biosciences) diluted in Tris-buffered saline with 0.1% Tween® 20 Detergent (TBST). Slides were coverslipped in Prolong Diamond Antifade Mountant (Thermo Fisher Scientific) and allowed to cure at room temperature overnight before imaging.

Multispectral imaging

All imaging was performed using a Vectra V.3.0.5 Automated Quantitative Pathology Imaging system (Akoya Biosciences). 20X resolution images covering the entire tumor for each patient sample were acquired using the 4',6-diamidino-2-phenylindole (DAPI), Fluorescein-5-isothiocyanate (FITC), Cy3, Texas Red, and Cy5 channels. Spectral unmixing was performed in inForm V.2.4.2 (Akoya Biosciences) using a spectral library created from signals acquired from single color controls.

Image analysis

Image analysis was performed in HALO V.3.0.1 (Indica Labs). Following unmixing, multispectral images were stitched together to create a single high-resolution multispectral image for each patient's tumor. In both nodal and in-transit samples, analysis was limited to intratumoral regions manually annotated by a clinical pathologist (AJC). Cell segmentation used an algorithm based on the presence of nuclear DAPI or SOX10 staining. Positivity thresholds for each marker were set based on cytoplasmic or nuclear staining intensity and were reviewed across all samples. Data for each cell's expression of all the markers and x and y locations within the tissue were stored in HALO for spatial analysis and exported for cell phenotyping in Spotfire V.7.11.1 (TIBCO). CD8+ T cells were phenotyped into eight groups based on their expression of CD39, CD103, and PD-1, and named sequentially from population 1 (P1) to population 8 (P8). In accordance with current literature,[29 30] CD39+CD103+PD-1+CD8+ T cells (P1) will be referred to as CD39+ tumor-resident memory CD8+ T cells (CD39+ Trm), and CD39−CD103−PD-1− CD8+ T cells (P8) as bystanders. Cell counts for each CD8+ T-cell phenotype were exported from Spotfire. Samples with <100 cells of a particular phenotype were removed from analysis of that phenotype. Further analyses were performed on P1, P5, and P8 due to their associations with recurrence and their biological significance.

Spatial analysis

Spatial analysis was performed using the HALO Spatial Analysis module (Indica Labs). Melanoma cells, CD8+ T cells, CD39+CD103+PD-1+CD8+ T cells, CD39-CD103+PD-1+ CD8+ T cells and CD39−CD103−PD-1−CD8+ T cells were phenotyped and plotted onto a spatial plot. The proximity analysis tool was used to identify the average distance of each CD8+ T-cell phenotype from melanoma cells, as well as the percentage of cells within each phenotype within 20 µm of a melanoma cell. Spatial data were exported for all three phenotypes in each spatial plot.

Statistical analysis

Statistical analysis of CD8+ T-cell population composition and spatial distribution was performed using an unpaired non-parametric Mann-Whitney test or paired non-parametric Friedman's test, respectively, in GraphPad Prism V.8. Samples were excluded from CD8+ T-cell population percentage composition analyses if they contained <100 CD8+ T cells. Correlation analysis was performed using corrplot package V.0.84 in R.

Clinical factors (as defined in table 2) and CD8+ T-cell populations were analyzed using a univariable Cox proportional hazard model. Given the limited number of events in the discovery cohort, a final predictive model was derived using multivariate models of predictive factors including CD8+ T cells and another clinical factor that maximized the predictive performance (C-statistics) of the model. The calibration performance of the model was done using calibration plots. Afterwards, external validation was performed by applying the coefficients and the baseline hazard of the discovery cohort to the independent cohort. Kaplan-Meier method and log-rank test were performed to determine the association between RFS and T-cell phenotypes including CD8+T cells (per mm^2, CD39+ Trm (% of CD8+) and bystanders (% of CD8+). Patients were divided into those above or below the median for each phenotype. All statistical analyses were performed using R V.3.6.3 and SAS V.9.4. P values of <0.05 were considered statistically significant in all analyses.

RESULTS

Patient characteristics

A consecutive discovery cohort of 103 patients with resected stage III melanoma—both nodal and in-transit metastases—who were treated with anti-PD-1-based adjuvant therapy were included. Baseline clinical data and melanoma tissue were collected for the eligible patients (table 1), with suitable tissue available for 91 patients. The median follow-up from the start of anti-PD-1 was 19.3 months (95% CI 15.4 to 21.5 months) across the cohort.

Table 2 Univariable and multivariable Cox regression of recurrence-free survival

	Univariable		Multivariable	
Variable	**HR (95% CI)**	**P value**	**HR (95% CI)**	**P value**
Gender				
Female	1	0.7880		
Male	1.10 (0.55 to 2.19)			
Age (years)				
≤60	1	0.1136		
>60	1.69 (0.88 to 3.25)			
Breslow thickness (mm)				
<1.0	1	0.3058		
1.0–2.0	0.42 (0.14 to 1.27)			
2.1–4.0	0.42 (0.15 to 1.20)			
>4.0	0.35 (0.11 to 1.11)			
Mitoses				
0/<1	1	0.1187		
1–3	0.10 (0.01 to 0.87)			
4–10	0.11 (0.01 to 0.97)			
>10	0.06 (0.01 to 0.61)			
BRAF				
NonV600E/WT	1	0.5124		
V600E	1.27 (0.63 to 2.56)			
Ulceration				
No	1	0.5294		
Yes	1.27 (0.60 to 2.67)			
Primary site				
Cutaneous	1	0.4699		
Acral	0.63 (0.09 to 4.64)			
Occult	0.54 (0.19 to 1.52)			
Stage III				
A/B	1	0.0375	1	0.5237
C/D	2.08 (1.04 to 4.15)		1.29 (0.59 to 2.82)	
Stage III detail				
Nodal only	1	0.5942		
ITM only	0.66 (0.23 to 1.88)			
Both nodal/ITM	0.49 (0.07 to 3.56)			
Time to stage III				
Concurrent	1	0.3919		
3–6 months	2.19 (0.63 to 7.67)			
6 months–1 year	1.30 (0.29 to 5.74)			
1–2 years	1.10 (0.36 to 3.35)			
>2 years	2.14 (0.94 to 4.85)			
LN status				
Microscopic	1	0.2765		
Macroscopic	1.48 (0.73 to 3.02)			
CLND performed				
No	1	0.0206	1	0.0267

Continued

Table 2 Continued

Variable	Univariable		Multivariable	
	HR (95% CI)	P value	HR (95% CI)	P value
Yes	2.69 (1.16 to 6.20)		2.85 (1.13 to 7.19)	
CLND site				
Neck	1	0.0029		
Axilla	0.51 (0.21 to 1.22)			
Groin	0.44 (0.14 to 1.40)			
Multiple	10.98 (1.98 to 60.94)			
Number of nodes				
0–1	1	0.0021		
2–3	1.12 (0.38 to 3.36)			
≥4	4.20 (1.76 to 10.04)			
Extranodal spread				
No	1	0.1794		
Yes	1.70 (0.78 to 3.68)			
White cell count				
Below median	1	0.4716		
Above median	1.29 (0.65 to 2.55)			
Neutrophil				
Below median	1	0.4531		
Above median	0.77 (0.38 to 1.53)			
Lymphocyte				
Below median	1	0.2501		
Above median	0.67 (0.34 to 1.33)			
Neutro:lympho ratio				
Below median	1	0.5433		
Above median	0.81 (0.41 to 1.61)			
Monocyte				
Below median	1	0.8997		
Above median	0.96 (0.48 to 1.90)			
Eosinophil				
Below median	1	0.6674		
Above median	0.86 (0.43 to 1.73)			
Basophil				
Below median	1	0.9861		
Above median	0.99 (0.49 to 2.00)			
CD8+ T cells (cells/mm^2)				
Below median	1	0.7760		
Above median	1.10 (0.56 to 2.16)			
CD39+CD103+PD-1+ % of CD8+ T cells				
Below median	1	0.0097	1	0.0036
Above median	0.39 (0.19 to 0.79)		0.32 (0.15 to 0.69)	
CD39-CD103-PD-1 % of CD8+ T cells				
Below median	1	0.1603		
Above median	1.64 (0.82, 3.28)			
CD8+ average distance to Mel				

Continued

Table 2 Continued

Variable	Univariable HR (95% CI)	Univariable P value	Multivariable HR (95% CI)	Multivariable P value
Below median	1	0.1171		
Above median	0.53 (0.24 to 1.17)			
CD39+CD103+PD-1+CD8+ average distance to Mel				
Below median	1	0.2473		
Above median	0.60 (0.26 to 1.42)			
CD39-CD103-PD-1-CD8+ average distance to Mel				
Below median	1	0.1311		
Above median	0.54 (0.25 to 1.20)			
%CD8+ >20 µm of Mel				
Below median	1	0.4267		
Above median	1.36 (0.64 to 2.91)			
%CD39+CD103+PD-1+CD8+ >20 µm of Mel				
Below median	1	0.6022		
Above median	0.80 (0.35 to 1.85)			
%CD39-CD103-PD-1-CD8+ >20 µm of Mel				
Below median	1	0.6283		
Above median	1.21 (0.56 to 2.62)			
PD-L1 status (>1%)				
Negative	1	0.5560		
Positive	0.81 (0.41 to 1.63)			

CLND, completion lymph node dissection; Mel, melanoma.

From the total cohort, 66 (64%) patients remained recurrence-free (RF) for the duration of the follow-up period and 37 (36%) experienced recurrence (R), with a 12-month RFS rate of 67.9% (95% CI 59.4% to 77.5%). The median time to recurrence was 5.3 months (95% CI 2.8 to 7.1 months). All recurrence-free patients had >10 months of follow-up.

Three phenotypically distinct CD8+ T-cell populations are significantly associated with recurrence

Staining and analysis were first performed in a discovery cohort (n=91) to examine the expression of CD39, CD103, and PD-1 on CD8+ T cells within melanoma tumor tissue, with individual melanoma cells identified by SOX10 expression (figure 1A).

T cell and CD8+ T-cell numbers were first quantified per square millimetre of tumor. T cell density was higher in recurrence-free patients, but not significantly so (R mean=1571 cells/mm^2, RF mean=2652 cells/mm^2; p=0.1278). As expected, CD8+ T-cell density was significantly higher in recurrence-free patients (R mean=517.6 cells/mm^2, RF mean=1476 cells/mm^2; p=0.0016; figure 1B,C). We then divided CD8+ T cells into eight phenotypically distinct populations based on their expression of CD39, CD103, and PD-1 (figure 1D). This classification encompasses all possible combinations of these three markers. From here, we examined the composition of the CD8+ T-cell compartment as a percentage of each of these eight populations (figures 1E,F and 2B and online supplemental figure 1). Based on their phenotype, P1 will be referred to as CD39+ tumor-resident memory CD8+ T cells (CD39+ Trm/P1), and P8 as bystanders/P8, in accordance with current literature.[29 30 34 35] Upon analysis, we found that three CD8+ T-cell populations were significantly different between recurrence and recurrence-free patients (figure 1E). The first of these, CD39+ Trm/P1, was characterized as CD39+CD103+PD-1+ and comprised a significantly higher proportion of the CD8+ T-cell compartment in recurrence-free patients (R mean=7.652%, RF mean=15.22%; p=0.0004). The second population, P8, was phenotyped as CD39-CD103-PD-1- and was significantly higher in recurrence patients (R mean=30.10, RF mean=15.18; p=0.0002). Finally, a smaller population, P5, phenotyped as CD39-CD103+PD-1+, was significantly higher in recurrence-free patients (R mean=5.009%, RF mean=8.629%; p=0.0008). We also performed correlation analysis of the CD8+ T-cell phenotypes, finding a negative correlation between CD39+ Trm/P1 and bystanders/P8 (figure 2A). Due to low numbers of patients treated with combination therapy (n=26), the impact of therapy type on CD8+ T-cell populations could not be adequately assessed (online supplemental figure 2).

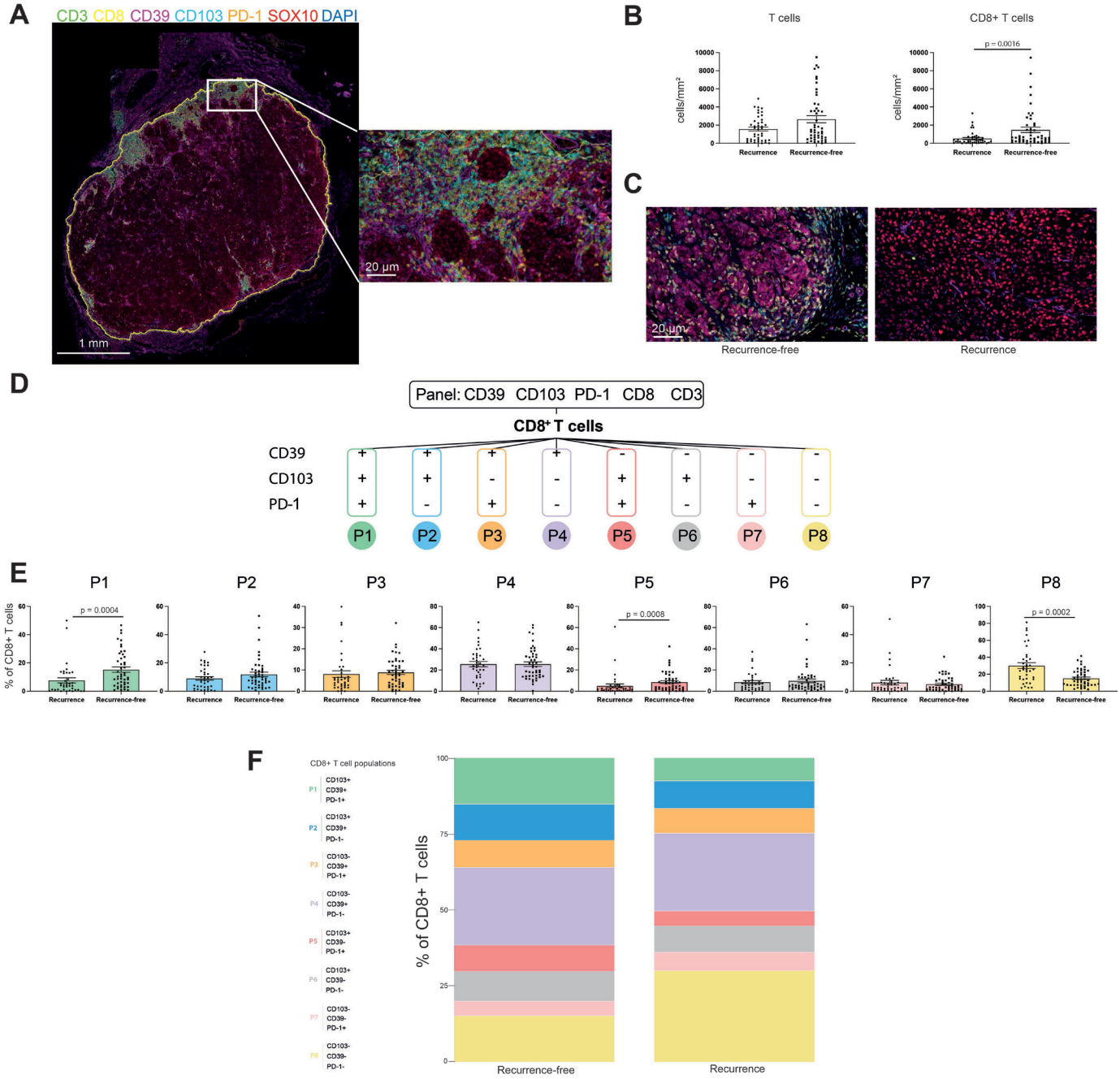

Figure 1 mIHC identifies significant CD8+ T-cell populations in adjuvant PD-1-treated patients with stage III melanoma. (A) mIHC was performed on pre-treatment stage III melanoma FFPE tissue from patients receiving adjuvant anti-PD-1 immunotherapy. Tumors were stained for CD3 (green), CD8 (yellow), CD39 (magenta), CD103 (cyan), PD-1 (orange), SOX10 (red) and DAPI (blue). Analysis was limited to intratumoral regions of tissue (highlighted in yellow). (B) Intratumoral T cells and CD8+ T cells CD8+ T cells were quantified per square millimetre of tumor and compared between recurrence patients and recurrence-free patients. Statistical differences were calculated using a non-parametric Mann-Whitney test (n=91). (C) Representative mIHC-stained FFPE sections from an RF patient and an R patient. (D) CD8+ T cells were divided into eight phenotypically distinct populations based on the expression of CD39, CD103 and PD-1. (E) Each population was quantified as a percentage of total CD8+ T cells in the discovery and validation cohorts. Recurrence-free patients have >10 months f/o. Samples with <100 CD8+T cells were excluded from this analysis (n=84). (F) Composition of the CD8+ T-cell compartment in Recurrence-free patients versus recurrence patients as a percentage of each population in all patients (n=84). FFPE, formalin-fixed paraffin-embedded; mIHC, multiplex fluorescent immunohistochemistry

CD39+ Trms localize within close proximity of melanoma cells

CD8+T cells, CD39+Trm/P1, P5, bystanders/P8, and melanoma cells underwent spatial analysis to determine the proximity of each CD8+ T-cell population to melanoma cells (figure 3A). First, we measured CD8+ T-cell infiltration by comparing the distance from a melanoma cell to the nearest CD8+ T cell, CD39+ Trm/P1, P5, or bystander/P8 between recurrence and recurrence-free

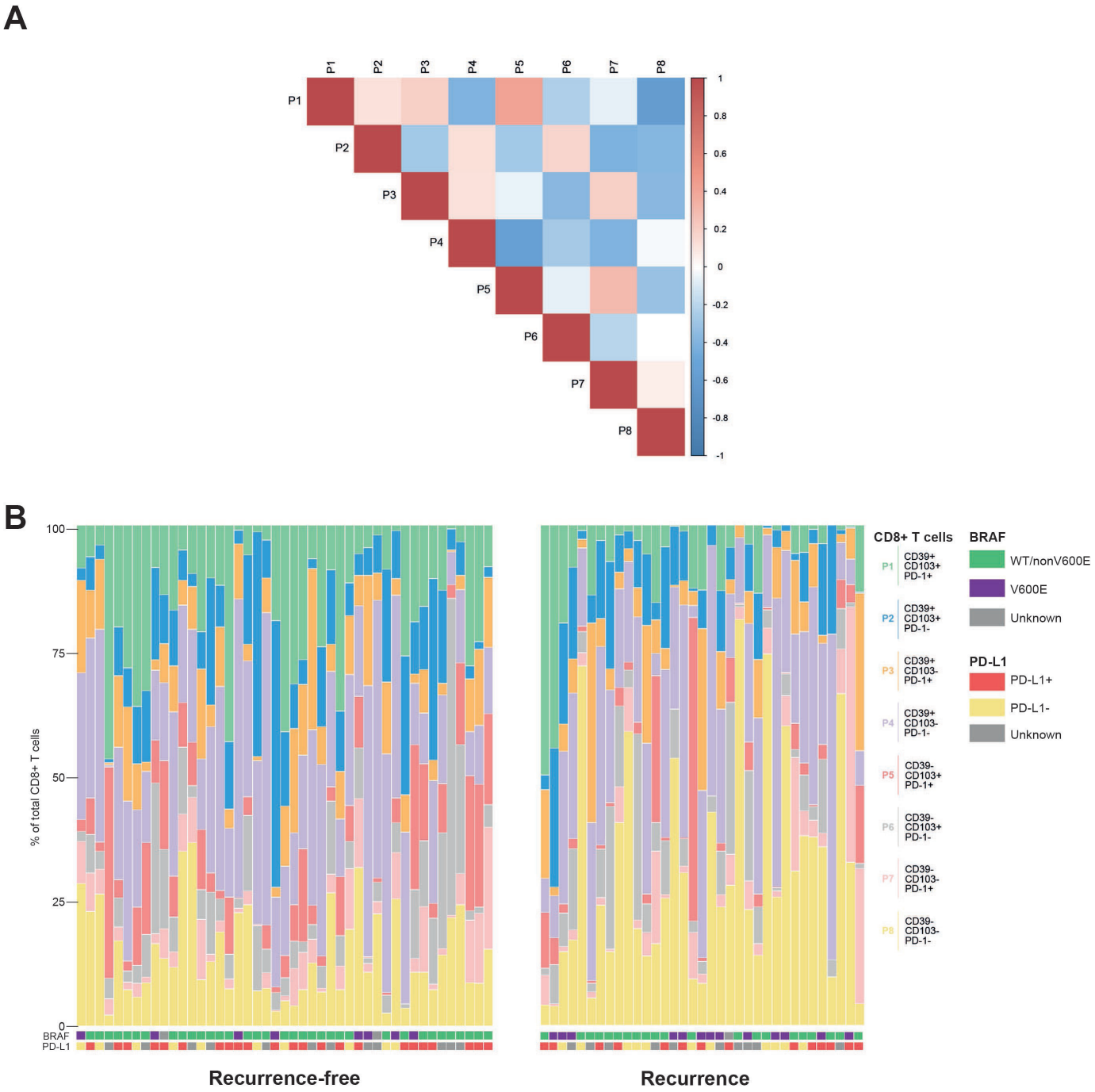

Figure 2 Patient CD8+ T-cell population and clinical profiles. (A) Correlation plot of all eight CD8+ T-cell phenotypes. Each population was expressed as a % of total CD8+ T cells and correlated with all other populations. (B) Patients were sorted from left to right by P1% of CD8+ T cells and split into recurrence-free patients and patients who had a recurrence. Profiles of the CD8+ T-cell compartment were generated for each patient. BRAF mutation and PD-L1 positivity information were also collected for each patient.

patients. As investigated previously by Gide *et al*,[36] we used 20 µm as a cut-off for proximity of each phenotype to melanoma. we found that a significantly higher percentage of melanoma cells were closer (within 20 µm) to CD39+ Trm in recurrence-free patients compared with recurrence patients (CD39+ Trm/P1 R mean=2.169%, CD39+ Trm/P1 RF mean=7.248%, p=0.0003; P5 R mean=4.654%, RF mean=5.778%, p=0.0747; bystanders/P8 R mean=6.555%, bystanders/P8 RF mean=6.159%, p=0.8628; figure 3B). By measuring the average distance from melanoma cells to each CD8+ T-cell phenotype, we found that melanoma cells were significantly closer to CD8+ and CD39+ Trm/P1 in recurrence-free than in recurrence patients (CD8 R mean=147.2 µm, CD8 RF mean=101.5 µm, p=0.0262; CD39+ Trm/P1 R mean=679.2 µm, CD39+ Trm/P1 RF mean=303.7 µm, p=0.0011; P5 R mean=493.2 µm, RF mean=252.6 µm, p=0.0564; bystanders/P8 R mean=278.9 µm, bystanders/

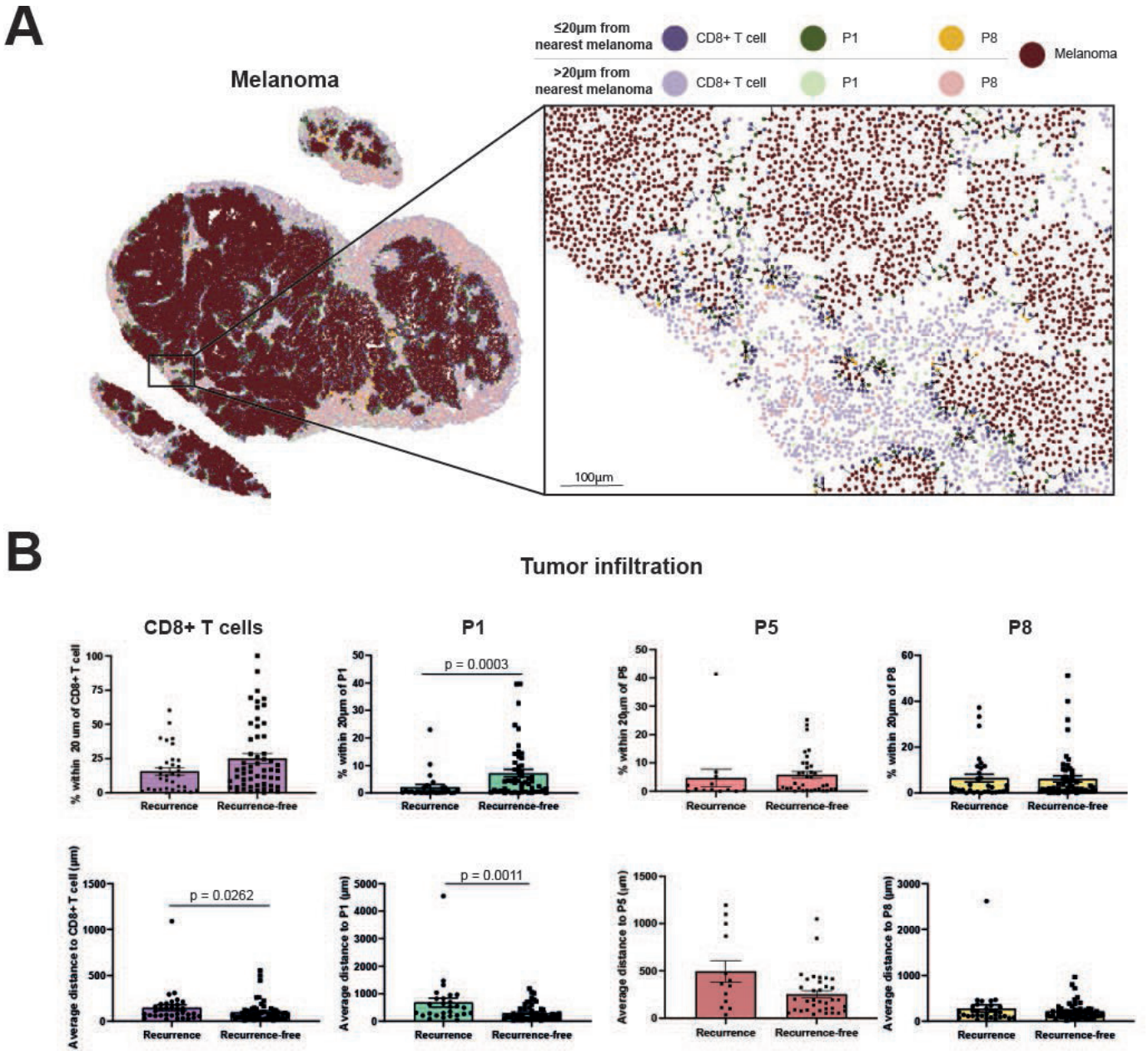

Figure 3 P1 proximity to melanoma is significantly closer than that of P5 or P8. (A) Spatial plot of melanoma, CD8+ T cells, P1 and P8. CD8+ T-cell populations within 20 µm proximity of melanoma cells are highlighted and line to nearest melanoma shown. (B) Spatial distribution of CD8+ T cells, P1, P5 and P8 in patients who had a recurrence (n=33) and patients who were recurrence-free (n=55). Percent of melanoma within 20 µm of each CD8+ T-cell population, and the average distance of melanoma to each population was quantified overall (n=84).

P8 RF mean=216.4 µm, p=0.7627; figure 3B). This indicates that of the three populations analyzed, CD39+ Trm/P1 is most likely to infiltrate and be in contact with the tumor cells of patients who remain recurrence-free. Based on similar previous studies,[22] we also measured the percentage of each population within 20 µm of melanoma. Due to the issues posed by low P5 cell numbers in the previous analysis, we chose to focus our remaining analysis on CD39+ Trm/P1 and bystanders/P8. We showed that a significantly higher percentage of CD39+ Trm/P1 were within 20 µm of melanoma than both total CD8+ T cells and bystanders/P8 (CD8 42.36%, CD39+ Trm/P1 45.35%, bystanders/P8 37.63%, CD8 vs CD39+ Trm/P1 p=0.0122, CD39+ Trm/P1 vs bystanders/P8 p<0.0001; online supplemental figure 3). We also measured the average distance of each T-cell phenotype to the nearest melanoma cell. This demonstrated that the distance from CD39+ Trms/P1 to the nearest melanoma cell was significantly closer than that of CD8+ T cells and bystanders/P8, while bystanders were additionally significantly further from melanoma cells than CD8+T cells (CD8+=5.38µm, CD39+ Trm/P1=36.67 µm, bystanders/P8=56.24 µm, CD8+vs CD39+ Trm/P1, p<0.0001, CD39+ Trm/P1 vs bystanders/P8 p<0.0001, CD8 vs bystanders/

P8, p=0.0173; online supplemental figure 4). Both measures found that CD39+ Trms/P1 were significantly closer to melanoma cells than bystanders/P8 and total CD8+ T cells.

High CD8+ T-cell density and high proportions of CD39+ Trm are associated with improved RFS time

We then performed RFS Kaplan-Meier analysis stratified by the median and quartiles of each CD8+ T-cell phenotype (figure 4A–C and online supplemental figures 4 and 5). Based on the median, there was no significant difference in RFS between patients with high and low total CD8+ T cells/mm^2 (1-year RFS high 63.4% vs low 64.2%; p=0.77). However, patients with high proportions of CD39+ Trm/P1 in their tumors had a significantly longer RFS than those with low proportions (1-year RFS high 78.1% vs low 49.9%; p=0.0073) with the median RFS not reached, and patients with the highest proportion of CD39+ Trm/P1 as quartiles had a 1-year RFS of 95% (online supplemental figure 4B). Median RFS for patients with low CD39+ Trm/P1 was 11.8 months and was not reached for patients with high CD39+Trm/P1. There was no association between bystander/P8 infiltration and RFS (1-year RFS high 54.6% vs low 73.2%, p=0.21). Univariable analysis of clinical and T-cell phenotypical data showed that more advanced stage of disease, performance of completion lymph node dissection (CLND), increased number of melanoma-positive lymph nodes and lower proportions of CD39+ Trm/P1 were associated with recurrence (table 2 and figure 4D). Lactate dehydrogenase (LDH) was not assessed in the univariate analysis as only one patient had an elevated baseline result. PD-L1 status was not significantly associated with recurrence regardless of the cut-off values used (table 2 and online supplemental figure 6). After excluding patients with missing clinical data, multivariate Cox regression analysis was then performed on 64 patients with clinical data combined with the proportion of intratumoral CD39+ Trms. Forward selection procedure was used to select the best model based on area under the curve (AUC) to classify patients at 1-year RFS from treatment start date. The final predictive multivariable model for recurrence included proportion of intratumoral CD39+ Trms/P1 (median=8.226%, p=0.0022), CLND performed (p=0.0267), and stage (p=0.5237) (table 2). Receiver operating characteristic curve analysis at 1-year RFS based on the multivariable model achieved an AUC of 75.9% (95% CI 65.3% to 86.5%). The model was applied to an independent validation cohort (n=33), with a median follow-up of 19.8 months (95% CI 15.4 months to 21.5 months) from start of therapy. All patients in this cohort received anti-PD-1 monotherapy, with 10 (25.6%) recurrence events. When applying the model to this cohort, the C-statistics became 69.5% (95% CI 48% to 91%) (figure 4E). The calibration plot comparing RFS Kaplan-Meier curves by risk groups indicated that the predictive model was well calibrated, with good agreement of the survival curves for all risk groups between the discovery and the validation cohorts (figure 4F).

DISCUSSION

Although adjuvant anti-PD-1 ICI therapy has significantly improved the RFS for patients with high-risk resected stage III melanoma,[1–3 12] many patients still recur. Despite many biomarkers for anti-PD-1 response being tested in the metastatic setting, none have translated into regular use in the clinic and improved patient care. In this study, we have performed a detailed and unique spatial and phenotypic characterization of the CD8+ T cell infiltrate in human stage III melanomas and have identified CD39+ tumor-resident memory CD8+ T cells (CD39+CD103+PD-1+, CD39+Trm/P1) as a critical population for RFS following immunotherapy. Of the CD8+ T cell populations studied, CD39+ Trm/P1 localize within the closest proximity to melanoma cells, suggesting their antitumor activity. Importantly, patients with a high proportion of this CD8+ T cell subpopulation had a significantly prolonged RFS compared with those with a low proportion (median 1-year RFS 79% vs 50%). A predictive multivariable model including the proportion of CD39+ Trms and clinical variables achieved an AUC of 75.9% in a discovery cohort and 69.5% in a separate validation cohort, demonstrating potential utility of this rapid and low-cost methodology to individualize risk of recurrence with adjuvant anti-PD-1.

Identifying T-cell subsets which initiate response to anti-PD-1 treatment and effectively control tumors has been the subject of intense research. A number of studies in different solid tumors pointed to a possible role for tumor-resident CD8+ T cells which express PD-1.[24] However, a sizeable fraction of CD8+ T cells infiltrating tumors, including resident CD8+ T cells, are not tumor specific.[29] Emerging data point to the expression of CD39 as a marker of tumor reactivity in humans.[29 30]

The current study highlights a critical subset of tumor-resident CD8+ T cells that could be crucial for response to anti-PD-1 treatment. In our study, CD39+ Trm/P1, which expresses CD39, CD103, and PD-1, made up a significantly higher proportion of CD8+ T cells infiltrating the tumors of recurrence-free patients, while bystander T cells/P8, which are negative for CD39, CD103, and PD-1, were increased in recurrence patients. Based on its phenotype, CD39+ Trm/P1 is likely to be tumor-resident, tumor antigen-specific, and highly differentiated, as well as responsive to anti-PD-1 therapy. Conversely, bystander T cells/P8 are negative for all three of these markers and are less likely to be tumor-reactive, raising questions as to their exact function in the TME and mechanisms of their recruitment. Our data also show that P5 (CD39–CD103+PD-1+) was also associated with RFS; however, to a lesser extent than P1. This suggests that P5 could be a tumor-resident population, but non-tumor reactive. Previous studies have shown that non-tumor-specific resident memory T cells could also contribute to tumor clearance[37]; however, their role in immunotherapy is unclear. While the exact antigen specificity of these populations remains in question, other studies have investigated the clonality of similar populations to CD39+ Trm/P1 and bystanders/P8. These have found that CD8+ T

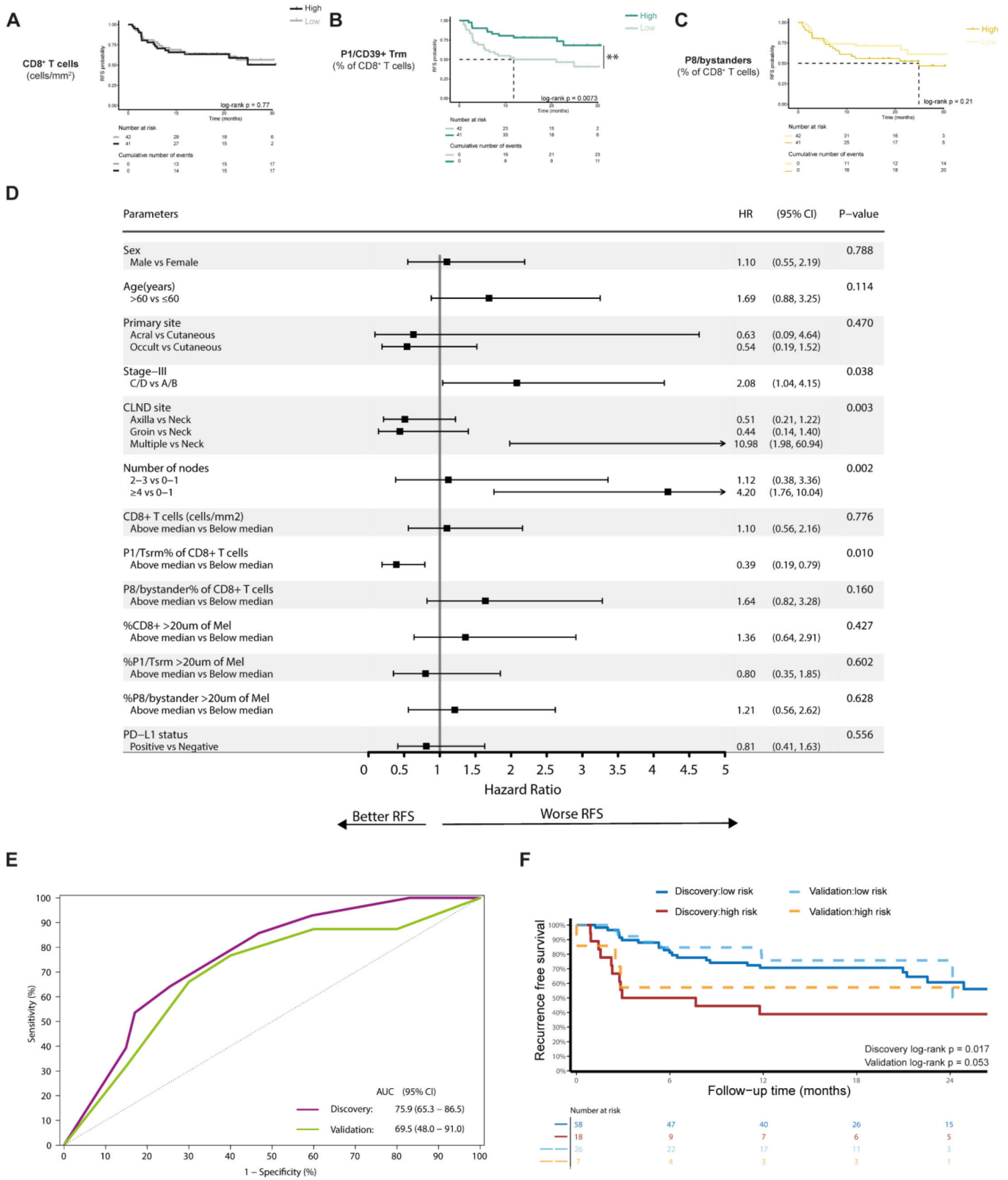

Figure 4 High P1/CD39+ Trm is significantly associated with RFS. Kaplan-Meier curves were plotted for patients with high CD8+ (A), P1 (B), P8 (C) cell counts against low counts. High versus low groups were determined by the median value for each cell population. Median RFS is shown where it is reached. Statistical differences were calculated using a log-rank test. (D) A forest plot was created from univariable Cox regression analysis. Horizontal bars indicate 95% CI. (E) The receiver operating characteristic curve shows the predictive capability of a predictive multivariable model for RFS including P1/CD39+ Trm% of CD8+ T cells, stage and CLND (discovery n=64, validation n=33). (F) Calibration plot compares RFS Kaplan-Meier curves for risk groups as defined by the MVA model in the discovery and validation cohorts. AUC, area under the curve; CLND, completion lymph node dissection; P1, population 1; P8, population 8; RFS, recurrence-free survival; Trm, tissue-resident memory cell.

cells similar to CD39+ Trm/P1 are more highly clonal, while cells similar to bystanders are less clonal, further supporting the notion that CD39+ Trm/P1 may have undergone tumor antigen-specific clonal expansion, while bystanders/P8 represent circulating non-tumor-specific T-cell populations.[29 38]

Our study used spatial analysis to provide some insight into the functionality of CD39+ Trm/P1 and bystander T cells/P8. We found that CD39+ Trm/P1 localized closer to melanoma cells, indicating its anti-tumor cytotoxicity.[22] On the other hand, bystanders/P8 were more distant. This further supports the idea that CD39+ Trm/P1 are more melanoma-reactive, while bystanders/P8 are non-tumor specific. Furthermore, Simoni *et al* found that tumor-infiltrating CD39- CD8+ T cells, while not specific for tumor antigens, can be specific for viral antigens.[29] Since bystanders/P8 do not localize closely to melanoma cells, the possibility that they could recognize non-tumor antigens in the TME and function as bystanders warrants investigation. Importantly, the role for CD39+ Trm/P1 in immunotherapy is particularly notable due to its expression of PD-1. As CD39+ Trm/P1 was likely to be reactivated by anti-PD-1 therapy, the finding that they localize in close proximity to melanoma cells suggests that they are well primed for a highly effective antitumor cytotoxic response. By contrast, P8 lacks PD-1 expression and is unlikely to contribute to this response. The roles of the other six CD8+ T-cell populations identified in our study are less clear. We observed positive correlations between populations based on PD-1 expression, suggesting that mechanisms of PD-1 expression may not be entirely linked to those of CD39 and CD103. Correlations also appear to form a gradient from CD39+ Trm/P1 to bystanders/P8, suggesting that cells with similar phenotypes are more likely to be found in the same tumors. We also observed a strong negative correlation between our P4 (CD39+CD103−PD-1−) and P5 populations (CD39−CD103+PD-1+), which is not unexpected due to their opposing phenotypes. Functional analyses would greatly complement these correlations and provide biological insights. Some direction is provided from Li *et al*'s investigation in human melanoma, finding that CD8+ T cells exist on a gradient from 'cytotoxic' to 'dysfunctional'.[39] The existence of this gradient, observed in both studies, suggests the possibility that P2–P7 in our study are transitional forms, and that CD39+ Trm/P1 and bystanders/P8 are the opposing endpoints of this transition. More work is needed to determine the eventual fate and functionality of P2–P7. An interesting note in this regard is that neoantigen expression by tumors is in constant flux and the CD8+ T-cell antigen repertoire tends to reflect this,[40] highlighting a potential rationale for the multiple CD8+ T-cell phenotypes observed in this study. Furthermore, recent studies suggest that in the context of ex vivo CD8+ T cells used for adoptive cell therapy, tumor-specific CD39− CD8+ T cells may act as a stem cell-like population which upregulates CD39 on differentiation, rather than as true bystanders.[41] However, further investigations of CD39− CD8+ T cells are needed in the tumors of ICI-treated patients.

While median RFS was not reached for high CD39+ Trm/P1 patients, low CD39+ Trm/P1 patients had a median RFS of only 11.8 months. Since our biomarker analysis was performed on pretreatment samples, using CD39+ Trm/P1 as a biomarker could allow for treatment decision-making prior to adjuvant therapy for patients likely to recur, for example, providing BRAF-targeted therapy rather than ICI in BRAF mutant patients with low CD39+ Trm[42] or neoadjuvant anti-PD-1+ anti-CTLA-4 for BRAF wt patients.[6 7 22] Indeed, a potential application of this biomarker could be in pre-treatment biopsies taken in the neoadjuvant setting.[43] Another possibility could be a more thorough investigation of drug targets in patients with low CD39+ Trm/P1, allowing for the administration of personalized therapies,[44] as well as increased monitoring following surgery. Furthermore, while CLND was included in our MVA model, it is often associated with other factors of nodal disease severity such as the number of nodes positive and macroscopic/microscopic disease. While we were unable to include all categories in our MVA model, inclusion of these categories in predictive modeling could be of importance for future studies.

The nature of our patient cohort imposed some limitations on the association of CD8+ T-cell populations with clinical data. PD-L1 status was not associated with recurrence in our cohort, which may be due to the high number of patients for whom PD-L1 status could not be accurately interpreted from IHC staining. We also observed a considerable imbalance in the PD-L1 status between the discovery and validation cohorts, which may reflect the reduced size of the validation cohort or differences in tissue suitability for PD-L1 staining. Nevertheless, since we did not find significant associations between PD-L1 status and CD8+ T-cell population composition, this imbalance between cohorts should not impact the findings of our study. Furthermore, BRAF mutations other than V600E were excluded from analysis since the majority of BRAF testing used VE1 IHC to detect the V600E mutation only. Our multivariable analysis was limited by low patient numbers in specific subgroups. The predictive capacity of CD39+ Trm/P1 specifically in the context of anti-PD-1 therapy remains to be fully established. To do so, CD39+ Trm/P1 would need to be assessed in the tumors of patients with melanoma receiving BRAF/MEK inhibitors or surgery alone. Finally, the small number of patients who did not receive PD-1 monotherapy but received combination with CTLA-4 would not impact the analysis and findings, as the anti-CTLA-4 was administered at low dose and low frequency and was recently shown to be equivalent to anti-PD-1 alone.[9]

This study highlights two phenotypically distinct CD8+ T-cell populations, CD39+ Trm (P1=CD39+CD103+PD-1+) and bystanders (P8=CD39−CD103−PD-1−). The phenotypes and associations with recurrence of these populations raise important questions regarding the recruitment and activity of CD8+ T cells in the TME. Furthermore,

given the results of our Kaplan-Meier and multivariable analyses, evaluation of CD39+ Trm in pretherapy melanoma tissue may have immediate clinical utility to predict which patients are likely to remain recurrence-free following anti-PD-1 therapy and to allow for treatment stratification in patients with stage III melanoma.

Author affiliations
[1]Melanoma Institute Australia, The University of Sydney, Sydney, New South Wales, Australia
[2]Faculty of Medicine and Health, The University of Sydney, Sydney, New South Wales, Australia
[3]The University of Bristol, Bristol Cancer Institute, University Hospitals Bristol and Weston NHS Foundation Trust, Bristol, UK
[4]Department of Tissue Oncology and Diagnostic Pathology, Royal Prince Alfred Hospital and NSW Health Pathology, Sydney, New South Wales, Australia
[5]Department of Melanoma and Surgical Oncology, Royal Prince Alfred Hospital; Mater Hospital, Sydney, New South Wales, Australia
[6]Westmead and Blacktown Hospitals, Sydney, New South Wales, Australia
[7]Royal North Shore and Mater Hospitals, Sydney, New South Wales, Australia

Twitter Umaimainthan Palendira @palendira and Richard A Scolyer @Twitter @ProfRScolyerMIA

Acknowledgements We thank the patients and families involved in this study for their contributions to our research. We are also grateful for ongoing support from colleagues at the Melanoma Institute Australia and the Charles Perkins Centre, University of Sydney.

Contributors Study design: GHA, CNO, IPdS, GVL and JSW. Sample and clinical data acquisition: CNO, JWC, KJN, JFT, IPdS, MSC, AMM and GVL. Pathology review: AJC. Experiments and data analysis: GHA. Statistical models and analysis: TA, IAV and SL. Data interpretation: GHA, CNO, SL, UP and JSW. Writing—original draft: GHA. Writing—review and editing: all authors. Supervision: UP, RAS, GVL and JSW. Funding: JFT, RAS and GVL. JSW acts as the guarantor of this study.

Funding This work was supported by a National Health and Medical Research Council of Australia (NHMRC) programme grant (APP1093017). GHA is supported by the Janet Ferguson MIA PhD Scholarship. KJN is supported by a scholarship from Melanoma Institute Australia. GHA and KJN are supported by scholarships from the University of Sydney. CNO and AJC were supported by Fellowships from Melanoma Institute Australia. JWC is supported by the Emma Betts MIA PhD Scholarship. IPdS is supported by a Cancer Institute NSW Early Career Fellowship. AMM is supported by Nicholas and Helen Moore and Melanoma Institute Australia. GVL, RAS and JSW are supported by NHMRC Fellowships. GVL is also supported by the University of Sydney Medical Foundation. Support from The Ainsworth Foundation, The CLEARbridge Foundation, Cameron Family and Lady Mary Fairfax Charitable Trust is also gratefully acknowledged.

Competing interests CNO reports non-financial support from Merck Sharp & Dohme. IPdS reports travel support by BMS and MSD, and speaker fees by Roche, BMS, MSD and Novartis. MSC reports personal fees from BMS, Merck Sharp & Dohme, Novartis, Roche, Amgen, Pierre-Fabre and Ideaya. JFT received honoraria for Advisory Board participation from Merck Sharpe & Dohme Australia and Bristol Myers Squibb Australia, honoraria and travel expenses from GlaxoSmithKline and Provectus, and conference attendance support from Novartis. AMM is on advisory boards for Bristol-Myers Squibb, Merck Sharpe & Dohme, Novartis Pharma AG, Roche, and Pierre-Fabre and QBiotics. RAS received fees for professional services from Evaxion, Provectus Biopharmaceuticals Australia, QBiotics, Merck Sharp & Dohme, GlaxoSmithKline Australia, Bristol-Myers Squibb, Dermpedia, Novartis, Myriad, NeraCare and Amgen. GVL is consultant advisor for Aduro Biotech, Amgen, Array Biopharma inc, Boehringer Ingelheim International GmbH, Bristol-Myers Squibb, Evaxion Biotech A/S, Hexel AG, Highlight Therapeutics S.L., Merck Sharpe & Dohme, Novartis Pharma AG, OncoSec, Pierre Fabre, QBiotics Group, Regeneron Pharmaceuticals, SkylineDX B.V. and Specialised Therapeutics Australia Pty Ltd. All remaining authors declared no competing interests.

Patient consent for publication Not applicable.

Ethics approval Baseline stage III melanoma resections, either in-transit metastasis or lymph node metastasis, were acquired for research with approval from the Sydney Local Health District Human Ethics Review Committee (protocol no X15-0454 & 2019/ETH06874 and protocol no X17-0312 & HREC/11/RPAH/32), and informed consent was obtained from each patient and from the MIA Biospecimen Tissue Bank.

Provenance and peer review Not commissioned; externally peer reviewed.

Data availability statement All data relevant to the study are included in the article or uploaded as supplementary information.

ORCID iDs
Grace Heloise Attrill http://orcid.org/0000-0001-8926-6582
John F Thompson http://orcid.org/0000-0002-2816-2496
Ines Pires da Silva http://orcid.org/0000-0003-3540-8906
Serigne Lo http://orcid.org/0000-0001-5092-5544
Umaimainthan Palendira http://orcid.org/0000-0002-1113-3306
Richard A Scolyer http://orcid.org/0000-0002-8991-0013
Georgina V Long http://orcid.org/0000-0001-8894-3545
James S Wilmott http://orcid.org/0000-0002-6750-5244

REFERENCES

1 Eggermont AMM, Blank CU, Mandala M, *et al*. Adjuvant pembrolizumab versus placebo in resected stage III melanoma. *N Engl J Med* 2018;378:1789–801.
2 Weber J, Mandala M, Del Vecchio M, *et al*. Adjuvant nivolumab versus ipilimumab in resected stage III or IV melanoma. *N Engl J Med* 2017;377:1824–35.
3 Eggermont AMM, Blank CU, Mandala M, *et al*. Longer follow-up confirms recurrence-free survival benefit of adjuvant pembrolizumab in high-risk stage III melanoma: updated results from the EORTC 1325-MG/KEYNOTE-054 trial. *J Clin Oncol* 2020;38:3925–36.
4 Eggermont AMM, Chiarion-Sileni V, Grob J-J, *et al*. Prolonged survival in stage III melanoma with ipilimumab adjuvant therapy. *N Engl J Med* 2016;375:1845–55.
5 Eggermont AMM, Chiarion-Sileni V, Grob J-J, *et al*. Adjuvant ipilimumab versus placebo after complete resection of stage III melanoma: long-term follow-up results of the European organisation for research and treatment of cancer 18071 double-blind phase 3 randomised trial. *Eur J Cancer* 2019;119:1–10.
6 Menzies AM, Amaria RN, Rozeman EA, *et al*. Pathological response and survival with neoadjuvant therapy in melanoma: a pooled analysis from the International neoadjuvant melanoma Consortium (INMC). *Nat Med* 2021;27:301–9.
7 Rozeman EA, Hoefsmit EP, Reijers ILM, *et al*. Survival and biomarker analyses from the OpACIN-neo and OpACIN neoadjuvant immunotherapy trials in stage III melanoma. *Nat Med* 2021;27:256–63.
8 Zimmer L, Livingstone E, Hassel JC, *et al*. Adjuvant nivolumab plus ipilimumab or nivolumab monotherapy versus placebo in patients with resected stage IV melanoma with no evidence of disease (IMMUNED): a randomised, double-blind, placebo-controlled, phase 2 trial. *Lancet* 2020;395:1558–68.
9 Long GV, Schadendorf D, Del Vecchio M. Adjuvant therapy with nivolumab (NIVO) combined with ipilimumab (IPI) vs NIVO alone in patients (PTS) with resected stage IIIB-D/IV melanoma (Checkmate 915). In American association of cancer research (AACR) annual meeting 2021.
10 Schachter J, Ribas A, Long GV, *et al*. Pembrolizumab versus ipilimumab for advanced melanoma: final overall survival results of a multicentre, randomised, open-label phase 3 study (KEYNOTE-006). *Lancet* 2017;390:1853–62.

11 Wolchok JD, Chiarion-Sileni V, Gonzalez R, *et al*. Overall survival with combined nivolumab and ipilimumab in advanced melanoma. *N Engl J Med* 2017;377:1345–56.
12 Ascierto PA, Del Vecchio M, Mandalá M, *et al*. Adjuvant nivolumab versus ipilimumab in resected stage IIIB-C and stage IV melanoma (CheckMate 238): 4-year results from a multicentre, double-blind, randomised, controlled, phase 3 trial. *Lancet Oncol* 2020;21:1465–77.
13 Erdag G, Schaefer JT, Smolkin ME, *et al*. Immunotype and immunohistologic characteristics of tumor-infiltrating immune cells are associated with clinical outcome in metastatic melanoma. *Cancer Res* 2012;72:1070–80.
14 Topalian SL, Hodi FS, Brahmer JR, *et al*. Safety, activity, and immune correlates of anti-PD-1 antibody in cancer. *N Engl J Med* 2012;366:2443–54.
15 Long GV, Larkin J, Ascierto PA. PD-L1 expression as a biomarker for nivolumab (NIVO) plus ipilimumab (IPI) and NIVO alone in advanced melanoma (MEL): a pooled analysis. *Ann Oncol* 2016;27:vi381.
16 Daud AI, Wolchok JD, Robert C, *et al*. Programmed death-ligand 1 expression and response to the anti-programmed death 1 antibody pembrolizumab in melanoma. *J Clin Oncol* 2016;34:4102–9.
17 Madore J, Vilain RE, Menzies AM, *et al*. PD-L1 expression in melanoma shows marked heterogeneity within and between patients: implications for anti-PD-1/PD-L1 clinical trials. *Pigment Cell Melanoma Res* 2015;28:245–53.
18 Carlino MS, Larkin J, Long GV. Immune checkpoint inhibitors in melanoma. *Lancet* 2021;398:1002–14.
19 Pires da Silva I, Wang KYX, Wilmott JS, *et al*. Distinct molecular profiles and immunotherapy treatment outcomes of V600E and V600K *BRAF*-mutant melanoma. *Clin Cancer Res* 2019;25:1272–9.
20 Larkin J, Chiarion-Sileni V, Gonzalez R, *et al*. Five-year survival with combined nivolumab and ipilimumab in advanced melanoma. *N Engl J Med* 2019;381:1535–46.
21 Pires Da Silva IED, Menzies AM, Newell F, *et al*. Comprehensive molecular profiling of metastatic melanoma to predict response to monotherapy and combination immunotherapy. *J Clin Oncol* 2019;37:9511.
22 Gide TN, Quek C, Menzies AM, *et al*. Distinct immune cell populations define response to anti-PD-1 monotherapy and Anti-PD-1/Anti-CTLA-4 combined therapy. *Cancer Cell* 2019;35:238–55.
23 Tumeh PC, Harview CL, Yearley JH, *et al*. PD-1 blockade induces responses by inhibiting adaptive immune resistance. *Nature* 2014;515:568–71.
24 Edwards J, Wilmott JS, Madore J, *et al*. CD103$^+$tumor-resident CD8$^+$ T cells are associated with improved survival in immunotherapy naive melanoma patients and expand significantly during anti-PD1 treatment. *Clin Cancer Res* 2018;24:3036–45.
25 Im SJ, Hashimoto M, Gerner MY, *et al*. Defining CD8+ T cells that provide the proliferative burst after PD-1 therapy. *Nature* 2016;537:417–21.
26 Carbone FR. Tissue-resident memory T cells and fixed immune surveillance in nonlymphoid organs. *J Immunol* 2015;195:17–22.
27 Banchereau R, Chitre AS, Scherl A, *et al*. Intratumoral CD103+ CD8+ T cells predict response to PD-L1 blockade. *J Immunother Cancer* 2021;9:e002231.
28 Masopust D, Soerens AG. Tissue-Resident T cells and other resident leukocytes. *Annu Rev Immunol* 2019;37:521–46.
29 Simoni Y, Becht E, Fehlings M, *et al*. Bystander CD8$^+$ T cells are abundant and phenotypically distinct in human tumour infiltrates. *Nature* 2018;557:575–9.
30 Duhen T, Duhen R, Montler R, *et al*. Co-expression of CD39 and CD103 identifies tumor-reactive CD8 T cells in human solid tumors. *Nat Commun* 2018;9:2724.
31 Oliveira G, Stromhaug K, Klaeger S, *et al*. Phenotype, specificity and avidity of antitumour CD8$^+$ T cells in melanoma. *Nature* 2021;596:119–25.
32 Long GV, Wilmott JS, Capper D, *et al*. Immunohistochemistry is highly sensitive and specific for the detection of V600E BRAF mutation in melanoma. *Am J Surg Pathol* 2013;37:61–5.
33 Paver EC, Cooper WA, Colebatch AJ, *et al*. Programmed death ligand-1 (PD-L1) as a predictive marker for immunotherapy in solid tumours: a guide to immunohistochemistry implementation and interpretation. *Pathology* 2021;53:141–56.
34 Thibaut R, Bost P, Milo I, *et al*. Bystander IFN-γ activity promotes widespread and sustained cytokine signaling altering the tumor microenvironment. *Nat Cancer* 2020;1:302–14.
35 Hoekstra ME, Bornes L, Dijkgraaf FE, *et al*. Long-distance modulation of bystander tumor cells by CD8$^+$ T cell-secreted IFNγ. *Nat Cancer* 2020;1:291–301.
36 Gide TN, Silva IP, Quek C, *et al*. Close proximity of immune and tumor cells underlies response to anti-PD-1 based therapies in metastatic melanoma patients. *Oncoimmunology* 2020;9:1659093.
37 Park SL, Buzzai A, Rautela J, *et al*. Tissue-resident memory CD8$^+$ T cells promote melanoma-immune equilibrium in skin. *Nature* 2019;565:366–71.
38 Yost KE, Satpathy AT, Wells DK, *et al*. Clonal replacement of tumor-specific T cells following PD-1 blockade. *Nat Med* 2019;25:1251–9.
39 Li H, van der Leun AM, Yofe I, *et al*. Dysfunctional CD8 T cells form a proliferative, dynamically regulated compartment within human melanoma. *Cell* 2019;176:775–89.
40 Verdegaal EME, de Miranda NFCC, Visser M, *et al*. Neoantigen landscape dynamics during human melanoma-T cell interactions. *Nature* 2016;536:91–5.
41 Krishna S, Lowery FJ, Copeland AR, *et al*. Stem-like CD8 T cells mediate response of adoptive cell immunotherapy against human cancer. *Science* 2020;370:1328.
42 Long GV, Hauschild A, Santinami M, *et al*. Adjuvant dabrafenib plus trametinib in stage III BRAF-mutated melanoma. *N Engl J Med* 2017;377:1813–23.
43 Amaria RN, Menzies AM, Burton EM, *et al*. Neoadjuvant systemic therapy in melanoma: recommendations of the International neoadjuvant melanoma Consortium. *Lancet Oncol* 2019;20:e378–89.
44 Edwards J, Tasker A, Pires da Silva I, *et al*. Prevalence and cellular distribution of novel immune checkpoint targets across longitudinal specimens in treatment-naïve melanoma patients: implications for clinical trials. *Clin Cancer Res* 2019;25:3247–58.